ROZPRAWY INŻYNIERSKIE • ENGINEERING TRANSACTIONS • 33, 3, 333–351, 1985
Polska Akademia Nauk • Instytut Podstawowych Problemów Techniki

STATE OF STRESS IN ANNULAR PRESTRESSED PLATE UNDER CREEP CONDITIONS

J. BIAŁKIEWICZ (KRAKÓW)

The solution of the problem of creep of an annular plate prestressed by a system of concentric cables is presented. The method of the solution is based on a double iterative algorithm. The problem of interaction of the cables and the influence of plane stress state on the state of bending of a plate have been solved by iterative methods.

1. Introduction

The processes taking place in prestressed plates are dependent on the physical and mechanical properties of the material of the plate and of the prestressing cables. The method of solution presented below is typical for nonmetallic plates (made from concrete or plastic) prestressed by a system of concentric cables. The usual phenomenon causing redistribution of stresses in normal temperatures is creep [1, 2]. In the case of concerte plates, during drying of the construction, shrinkage takes place. The extent of the shrinkage depends on hydrothermal conditions of the environment [3].

The work of prestressed cables is usually limited to the linear-elastic range. However, if the designed stress level in cables is close to the yield point, the plastic-visco-elastic model of the material for the prestressing cables should be applied [4].

The paper is a continuation of problems studied by the author in [5]. The new elements of the present paper are:

the influence of bending upon the longitudinal forces,

the algorithm of solution of an annular disc prestressed by a system of concentric cables,

the algorithm of the analysis of an annular plate after rejection of the stiffness principle (the second order theory), and

the numerical example of the analysis of an annular plate prestressed by six cables.

Assuming the distribution of cables to be uniform, the magnitudes of individual prestressing forces are determined. The problems of optimal prestressing [6] remains unsolved.

2. Formulation of the problem

A model of the plate material will be assumed according to the physical relation of the Boltzman infinitesimal theory [7, 8]

$$\mathbf{T}(\tau) = \{E_0(\tau)\,\mathrm{tr}\,\mathbf{E}(\tau) - \int_1^\tau \mathrm{tr}\,\mathbf{E}(\tau')\,E_0(\tau')\,R_0(\tau,\tau')\,d\tau'\}\,\mathbf{1} + \tag{2.1}$$
$$+2G(\tau)\,\mathbf{E}'(\tau) - 2\int_1^\tau \mathbf{E}'(\tau')\,G(\tau')\,R_c(\tau,\tau')\,d\tau'.$$

The symbols used in the equation denote: $\mathbf{T}(\tau)$ — Cauchy's stress tensor, $\mathbf{E}(\tau)$ — the strain tensor, $\mathbf{E}'(\tau)$ — the strain deviator. The magnitudes E_0, $G(\tau)$, $R_0(\tau,\tau')$, $R_c(\tau,\tau')$ are scalar material functions of the loading time τ and the age of the material τ'. Equation (2.1) is presented in dimensionless variables. In the formulated initial-boundary problem, the stress $\mathbf{T}(\tau)$ and strain $\mathbf{E}(\tau)$ tensors will be written in a cylindrical coordinate system $\{\varrho,\theta,\zeta\}$.

The governing set of equations will be written after rejection of the stiffness principle (the second order theory). This makes it possible to account for the influence of plane stress ("disc") forces (caused by prestressing) on the plate deflection [9, 10]. The equilibrium equations of the horizontal n_ϱ, n_Θ and vertical forces q_ϱ and moments m_ϱ, m_Θ, with vectors tangent to the deflected surface of the plate, can be written in the form

$$n_{\varrho,\varrho} + \frac{1}{\varrho}(n_\varrho - n_\Theta) = 0, \tag{2.2}$$

$$\varrho q_{\varrho,\varrho} + q_\varrho = \varrho\bar{q}, \tag{2.3}$$

$$m_{\varrho,\varrho} + \frac{1}{\varrho}(m_\varrho - m_\Theta) + n_\varrho\,\bar{w}_{,\varrho} = q_\varrho, \tag{2.4}$$

where $\bar{q}$ and $\bar{w}$ denote the dimensionless load and deflection functions.

According to the theory of thin plates, the constitutive equation (2.1) will be written just as for the plane stress and strain states,

$$s_\varrho = \frac{2}{3}S_c(2\varepsilon_\varrho - \varepsilon_\theta) + S_0(\varepsilon_\varrho + \varepsilon_\theta), \tag{2.5}$$

$$s_\Theta = \frac{2}{3}S_c(2\varepsilon_\Theta - \varepsilon_\varrho) + S_0(\varepsilon_\varrho + \varepsilon_\Theta), \tag{2.6}$$

where, to simplify the notation, the integral operators have been defined:

$$S_c(s) = G(\tau)\,s(\tau) - \int_1^\tau s(\tau')\,G(\tau')\,R_c(\tau,\tau')\,d\tau', \tag{2.7}$$

$$S_0(s) = E_0(\tau)\, s(\tau) - \int_1^\tau s(\tau')\, E_0(\tau')\, R_0(\tau, \tau')\, d\tau'. \tag{2.8}$$

The magnitudes s_ϱ, s_Θ and $\varepsilon_\varrho, \varepsilon_\Theta$ denote the radial and circumferential components of stress $\mathbf{T}(\tau)$ and strain $\mathbf{E}(\tau)$ tensors. The dimensionless material function $G(\tau)$ and $E_0(\tau)$ are given in the paper [5].

The inverse form of the physical equations (2.5) and (2.6) will be particularly useful in the analysis of the plane stress state

$$\varepsilon_\varrho = \frac{1}{6} L_c(2s_\varrho - s_\theta) + \frac{1}{9} L_0(s_\varrho + s_\theta), \tag{2.9}$$

$$\varepsilon_\Theta = \frac{1}{6} L_c(2s_\Theta - s_\varrho) + \frac{1}{9} L_0(s_\varrho + s_\Theta). \tag{2.10}$$

This form has been written using the integral operators inverse to (2.7) and (2.8),

$$L_c(s) = \frac{1}{G(\tau)} \left[s(\tau) + \int_1^\tau s(\tau')\, \bar{K}_c(\tau, \tau')\, d\tau' \right], \tag{2.11}$$

$$L_0(s) = \frac{1}{E_0(\tau)} \left[s(\tau) + \int_1^\tau s(\tau')\, \bar{K}_0(\tau, \tau')\, d\tau' \right]. \tag{2.12}$$

A nondilatational $\bar{K}_c(\tau, \tau')$ and dilatational $\bar{K}_0(\tau, \tau')$ kernels depend on Poisson's coefficients $\mu(\tau)$, $\nu(\tau, \tau')$, and the general kernel of Eq. (2.1):

$$\bar{K}_c(\tau, \tau') = \frac{1 + \nu(\tau, \tau')}{1 + \mu(\tau)}\, \bar{K}(\tau, \tau'), \qquad \bar{K}_0(\tau, \tau') = \frac{1 - 2\nu(\tau, \tau')}{1 - 2\mu(\tau)}\, \bar{K}(\tau, \tau'). \tag{2.13}$$

The analytical form of the kernel $\bar{K}(\tau, \tau')$ will be further referred to the commonly applied creep theories of concrete [11, 12] and chosen plastics. The material functions $R_c(\tau, \tau')$ and $R_0(\tau, \tau')$ will be calculated as the resolvents of the integral equations (2.9) and (2.10) for the assumed form of the kernel $\bar{K}(\tau, \tau')$.

3. Differential-functional plate equation

Negligible dependence of Poisson's ratios (2.13) on time for most of the constructional materials yields the assumption

$$\mu(\tau) = \nu(\tau, \tau') = \mu = \text{const}, \tag{3.1}$$

what leads to

$$R_c(\tau, \tau') = R_0(\tau, \tau') = R(\tau, \tau'). \tag{3.2}$$

In this way, practical application of the solutions is not too narrow. Equations (2.5) and (2.6) for the plate state, after additional expression of the components of the strain tensor by the function of deflection $\bar{w}$ (the Kirchhoff assumption), can be written in the integral form

$$m_\varrho = -\frac{4}{3(1-\mu)} S_c\left(\bar{w}_{,\varrho\varrho} + \mu \frac{1}{\varrho}\bar{w}_{,\varrho}\right), \tag{3.3}$$

$$m_\Theta = -\frac{4}{3(1-\mu)} S_c\left(\frac{1}{\varrho}\bar{w}_{,\varrho} + \mu \bar{w}_{,\varrho\varrho}\right), \tag{3.4}$$

where

$$\left.\begin{matrix} m_\varrho \\ m_\Theta \end{matrix}\right\} = \int_{-1}^{1} \left.\begin{matrix} s_\varrho \\ s_\Theta \end{matrix}\right\} \zeta \, d\zeta. \tag{3.5}$$

The transversal force expressed by the function of deflection $\bar{w}$ results from the equilibrium Eq. (2.4) after substituting m_ϱ and m_Θ for (3.3) and (3.4);

$$q_\varrho = -\frac{4}{3(1-\mu)} S_c\left[(\nabla^2 \bar{w})_{,\varrho}\right] + n_\varrho \bar{w}_{,\varrho}. \tag{3.6}$$

The differential-functional plate equation will be obtained as a result of introduction of Eq. (3.6) into Eq. (2.3). Taking also into consideration the constant plane (disc) stress distribution across the thickness caused by prestressing Eq. (2.2),

$$s_\varrho^T = \frac{1}{2} n_\varrho, \qquad s_\Theta^T = \frac{1}{2} n_\Theta, \tag{3.7}$$

the differential-functional plate equation can be written as

$$\nabla^2 \nabla^2 \bar{w} - \frac{3}{4}(1-\mu) L_c\left[\bar{q} + \frac{2}{\varrho} s_\Theta^T \bar{w}_{,\varrho} + 2 s_\varrho^T \bar{w}_{,\varrho\varrho}\right] = 0. \tag{3.8}$$

In this equation, besides the unknown function of deflection $\bar{w}(\varrho, \tau)$, the unknown disc stresses s_ϱ^T and s_Θ^T appear. Since the equilibrium conditions of forces acting in the middle surface of the plate (2.2) are independent, the solution of the disc problem will be presented first.

4. Prestressing stresses

The solution of the disc state problem of the plate, caused by prestressing, will be presented by applying the statical approach. This method has been

discussed in detail in paper [5]. In the considered plane, axially-symmetrical problem, the elastic-viscous-elastic analogy takes place [11]. The function of the radial stress is the solution of the equation

$$\varrho s_{\varrho,\varrho\varrho} + 3 s_{\varrho,\varrho} = 0. \tag{4.1}$$

The algorithm of the solution presented below will be illustrated by an example of creep analysis of an annular plate in compliance with the scheme shown in Fig. 1. The geometry of the plate is determined by: the radius of the cantilever column R_1, the external radius R_2 and the constant thickness $2h$. The magnitude $q(r)$ is a function of the useful load, whereas $p^{(i)}$ denotes the pressure exerted by the i-th prestressing cable ($i = 1, 2, \ldots, n$) the route of which coincides with a circle of radius $R^{(i)}$.

A static scheme of division of the plate along the i-th cable route is shown in Fig. 2. The load functions of the external edge (a) and hole (b) of the plate, after assumption that the cables work in the linear elastic region,

$$\bar{p}^{(i)}(\tau) = \bar{a}_1^{(i)} + \bar{a}_2^{(i)}\, \bar{u}^{(i)}(\tau) \tag{4.2}$$

have the form

$$\bar{p}_c^{(i)}(\tau) = \bar{a}_{21}^{(i)} + \bar{a}_{22}^{(i)} [\bar{u}_{RC}^{(i)}(\tau) + \bar{u}_R^{(i)}(\tau)], \tag{4.3}$$

$$\bar{p}_r^{(i)}(\tau) = \bar{a}_{11}^{(i)} + \bar{a}_{12}^{(i)} [\bar{u}_{RC}^{(i)}(\tau) + \bar{u}_R^{(i)}(\tau)]. \tag{4.4}$$

A sum of the components: $\bar{u}_{RC}^{(i)}(\tau)$ (the function describing the creep of the plate under the influence of one cable the route of which coincides with a circle of radius $r = R^{(i)}$) and $\bar{u}_R^{(i)}$ (the function of displacement produced by other

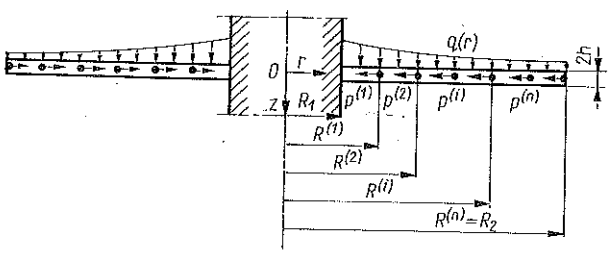

FIG. 1.

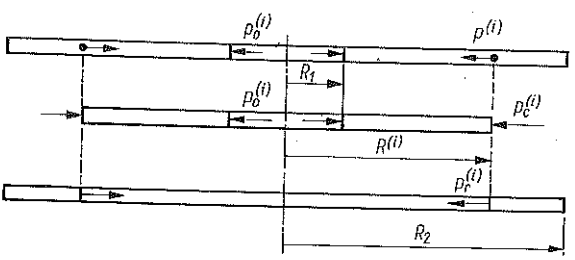

FIG. 2.

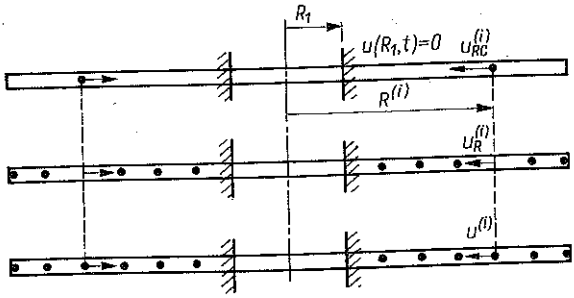

FIG. 3.

cables) of the vector $\vec{u}^{(i)}(\tau)$ is presented in Fig. 3. The dimensionless magnitudes in Eqs. (4.2)–(4.3) are expressed by

$$\vec{p}^{(i)}(\tau) = \frac{1}{s_0} p^{(i)}(\tau), \qquad \vec{u}^{(i)}(\tau) = \frac{1}{h} u^{(i)}(\tau),$$

$$\vec{a}_1^{(i)}(\tau) = \frac{1}{s_0} a_1^{(i)}(\tau), \qquad \vec{a}_2^{(i)}(\tau) = \frac{h}{s_0} a_2^{(i)}(\tau), \tag{4.5}$$

where

$$u^{(i)}(t) = u(R^{(i)}, t). \tag{4.6}$$

Two algebraic equations for the coefficients of the load distribution $\vec{a}_{kl}^{(i)}$ are given by the relations

$$\vec{a}_{11}^{(i)} + \vec{a}_{21}^{(i)} = \vec{a}_1^{(i)},$$
$$\vec{a}_{12}^{(i)} + \vec{a}_{22}^{(i)} = \vec{a}_2^{(i)}. \tag{4.7}$$

Two further equations for the coefficients $\vec{a}_{kl}^{(i)}$ are written on the basis of the continuity conditions for the function of radial displacement at the points $r = R^{(i)}$. Assuming, at this stage, the values of these coefficients as known, the static boundary conditions can be presented separately for

the region (a)

$$s_\varrho^{(i)}(\varrho_1, \tau) = -\vec{p}_0^{(i)}(\tau),$$
$$s_\varrho^{(i)}(\varrho^{(i)}, \tau) = -\vec{p}_c^{(i)}(\tau), \tag{4.8}$$

and region (b) of the plate

$$s_\varrho^{(i)}(\varrho^{(i)}, \tau) = \vec{p}_r^{(i)}(\tau),$$
$$s_\varrho^{(i)}(\varrho_2, \tau) = 0, \tag{4.9}$$

where $\vec{p}_0^{(i)}$ is reaction pressure produced by the i-th cable in a fixed point, Fig. 2

$$\vec{p}_0^{(i)} = \frac{1}{s_0} p_0^{(i)}(\tau), \tag{4.10}$$

and ϱ_1, ϱ_2 denote dimensionless internal and external radii of the plate

$$\varrho_1 = \frac{R_1}{h}, \quad \varrho_2 = \frac{R_2}{h}. \tag{4.11}$$

From the solution of differential equation (4.1), with the boundary conditions (4.8) and (4.9), the radial and circumferential stresses can be obtained in the regions of

the plate (a)

$$\left.\begin{matrix} s_\varrho^{(i)} \\ s_\theta^{(i)} \end{matrix}\right\} = \frac{\bar{p}_0^{(i)} - \bar{a}_{21}^{(i)} - \bar{a}_{22}^{(i)} [\bar{u}_{RC}^{(i)} + \bar{u}_R^{(i)}]}{1 - \left[\frac{\varrho_1}{\varrho^{(i)}}\right]^2} \left[1 \mp \left(\frac{\varrho_1}{\varrho}\right)^2\right] - \bar{p}_0^{(i)} \tag{4.12}$$

and the plate (b)

$$\left.\begin{matrix} s_\varrho^{(i)} \\ s_\theta^{(i)} \end{matrix}\right\} = \frac{-\bar{a}_{11}^{(i)} - \bar{a}_{12}^{(i)} [\bar{u}_{RC}^{(i)} + \bar{u}_R^{(i)}]}{1 - \left[\frac{\varrho^{(i)}}{\varrho_2}\right]^2} \left[1 \pm \left(\frac{\varrho^{(i)}}{\varrho}\right)^2\right] + \bar{a}_{11}^{(i)} + \bar{a}_{12}^{(i)} [\bar{u}_{RC}^{(i)} + \bar{u}_R^{(i)}]. \tag{4.13}$$

The relations (4.12) and (4.13) indicate the dependence of stresses on the displacement functions $\bar{u}_{RC}^{(i)}$ and $\bar{u}_R^{(i)}$ at the points of the plate where the cables are placed. These functions will be determined by means of the constitutive equation (2.1) written for a fixed value of radial variable $\varrho = \varrho^{(i)}$.

5. Function of radial displacement

The material function $\bar{K}(\tau, \tau')$ is usually found to be nonlinear [14, 15, 16]. In the present paper it is taken as a nonlinear, degenerated function [12, 13]

$$\bar{K}(\tau, \tau') = f_1(\tau) g_1(\tau') + f_2(\tau) g_2(\tau'), \tag{5.1}$$

where

$$f_1(\tau) = \bar{E}(\tau), \quad f_2(\tau) = \bar{E}(\tau) e^{-\gamma\tau},$$

$$g_1(\tau') = \frac{1}{\bar{E}^2(\tau')} \frac{d\bar{E}(\tau')}{d\tau'} - \frac{d\bar{\varphi}(\tau')}{d\tau'}, \quad g_2(\tau) = \left[\frac{d\bar{\varphi}(\tau')}{d\tau'} + \gamma\bar{\varphi}(\tau')\right] e^{\gamma\tau'}. \tag{5.2}$$

The dimensionless ageing $\bar{\varphi}(\tau)$ and Young's modulus $E(\tau)$ functions appearing in Eq. (5.2) will be taken into as follows [15]:

$$\bar{\varphi}(\tau') = C_0 + \frac{A}{\tau'}, \quad \bar{E}(\tau) = E_0 (1 - \beta e^{-\alpha\tau}). \tag{5.3}$$

The physical properties of the material are identified by means of the constants: $C_0, A, E_0, \alpha, \beta$ and γ.

The integral physical relation (2.10), in case of the kernel determined by the formula (5.1), after double differentiation, can be replaced by a differential equation. This equation with two initial conditions constitutes the initial problem [5] for unknown functions of displacement $\bar{u}_{RC}^{(i)}$ and reaction pressure $\bar{p}_0^{(i)}$

$$\partial_\tau^2 s_\vartheta^{(i)}(\varrho,\tau)-\mu\partial_\tau^2 s_\varrho^{(i)}(\varrho,\tau)+\left\{\gamma\left[1+\bar{E}(\tau)\,\bar{\varphi}(\tau)\right]-\frac{1}{\bar{E}(\tau)}\,\partial_\tau \bar{E}(\tau)\right\}\left[\partial_\tau s_\vartheta^{(i)}(\varrho,\tau)-\mu\partial_\tau s_\varrho^{(i)}(\varrho,\tau)\right]= \tag{5.4}$$
$$=\bar{E}(\tau)\left[\frac{1}{\varrho}\,\partial_\tau^2 \bar{u}^{(i)}(\varrho,\tau)+\frac{\gamma}{\varrho}\,\partial_\tau \bar{u}^{(i)}(\varrho,\tau)\right],$$

$$\bar{E}(1)\frac{1}{\varrho}\,\bar{u}^{(i)}(\varrho,1)=s_\vartheta^{(i)}(\varrho,1)-\mu s_\varrho^{(i)}(\varrho,1), \tag{5.5}$$

$$\bar{E}(1)\frac{1}{\varrho}\,\partial_\tau \bar{u}^{(i)}(\varrho,1)=\partial_\tau s_\vartheta^{(i)}(\varrho,1)-\mu\partial_\tau s^{(i)}(\varrho,1)+\frac{1}{\varrho}\,\gamma\bar{\varphi}(1)\,\bar{E}^2(1)\,\bar{u}^{(i)}(\varrho,1). \tag{5.6}$$

The stresses $s_\varrho^{(i)}$ and $s_\vartheta^{(i)}$ occurring in Eqs. (5.4)–(5.6) are determined separately for the regions (a) (4.12) and (b) (4.13) of the plate. In particular, two initial problems for two unknown functions: $\bar{p}_0^{(i)}$ and $\bar{u}_{RC}^{(i)}$ from the interval (a) follow. The first of them will be formulated by substituting into Eqs. (5.4)–(5.6) the stresses (4.12). Taking into account the boundary condition

$$\bar{u}(\varrho_1,\tau)=0. \tag{5.7}$$

Equations (5.4)–(5.6) can be written in the form

$$\partial_\tau^2 \bar{p}_0^{(i)}+f(\tau)\,\partial_\tau \bar{p}_0^{(i)}=\frac{2\bar{a}_{22}^{(i)}}{D_1^{(i)}}\left[\partial_\tau^2 \bar{u}_{RC}^{(i)}+\partial_\tau^2 \bar{u}_R^{(i)}+f(\tau)\left(\partial_\tau \bar{u}_{RC}^{(i)}+\partial_\tau \bar{u}_R^{(i)}\right)\right], \tag{5.8}$$

$$\partial_\tau \bar{p}_0^{(i)}(1)=\frac{2\bar{a}_{22}^{(i)}}{D_1^{(i)}}\left[\partial_\tau \bar{u}_{RC}^{(i)}(1)+\partial_\tau \bar{u}_R^{(i)}(1)\right], \tag{5.9}$$

$$\bar{p}_0^{(i)}(1)=\frac{2}{D_1^{(i)}}\left\{\bar{a}_{22}^{(i)}\left[\bar{u}_{RC}^{(i)}(1)+\bar{u}_R^{(i)}(1)\right]+\bar{a}_{21}^{(i)}\right\}, \tag{5.10}$$

where

$$f(\tau)=\gamma\left[1+\bar{E}_0\left(C_0+\frac{A}{\tau}\right)(1-\beta e^{-\alpha\tau})\right]-\frac{\alpha\beta e^{-\alpha\tau}}{1-\beta e^{-\alpha\tau}}. \tag{5.11}$$

The second initial problem for the region (a) of the plate follows from Eqs. (5.4)–(5.6) after substitution of Eq. (4.12) with the fixed value of the radius $\varrho = \varrho^{(i)}$

$$\partial_\tau^2 \bar{p}_0^{(i)} + f(\tau)\,\partial_\tau \bar{p}_0^{(i)} = -\frac{\bar{a}_{22}^{(i)} D_2^{(i)}}{D_3^{(i)}} \{\partial_\tau^2 \bar{u}_{RC}^{(i)} + \partial_\tau^2 \bar{u}_R^{(i)} + f(\tau)\,[\partial_\tau \bar{u}_{RC}^{(i)} + \partial_\tau \bar{u}_R^{(i)}]\} + \frac{\bar{E}}{\varrho^{(i)}} (\partial_\tau^2 \bar{u}_{RC}^{(i)} + \gamma \partial_\tau \bar{u}_{RC}^{(i)}) \frac{1}{D_3^{(i)}}, \tag{5.12}$$

$$\partial_\tau \bar{p}_0^{(i)}(1) = -\frac{\bar{a}_{22}^{(i)} D_2^{(i)}}{D_3^{(i)}} [\partial_\tau \bar{u}_{RC}^{(i)}(1) + \partial_\tau \bar{u}_R^{(i)}(1)] + \frac{1}{\varrho^{(i)} D_3^{(i)}} [\bar{E}(1)\,\partial_\tau \bar{u}_{RC}^{(i)}(1) - g(1)\,\bar{u}_{RC}^{(i)}(1)], \tag{5.13}$$

$$\bar{p}_0^{(i)}(1) = -\frac{D_2^{(i)}}{D_3^{(i)}} \{[\bar{u}_{RC}^{(i)}(1) + \bar{u}_R^{(i)}(1)]\,\bar{a}_{22}^{(i)} + \bar{a}_{21}^{(i)}\}, \tag{5.14}$$

where

$$g(\tau) = \gamma E_0^2 \left(C_0 + \frac{A}{\tau}\right)(1 - \beta e^{-\alpha\tau}). \tag{5.15}$$

In both sets of Eqs. (5.8)–(5.10) and (5.12)–(5.14), the magnitudes characterizing the geometry of the interval (a) of the plate are denoted by

$$D_1^{(i)} = 2 - (1-\mu)\left[1 - \left(\frac{\varrho_1}{\varrho^{(i)}}\right)^2\right], \quad D_2^{(i)} = \mu - \frac{1 + \left(\frac{\varrho_1}{\varrho^{(i)}}\right)^2}{1 - \left(\frac{\varrho_1}{\varrho^{(i)}}\right)^2},$$

$$D_3^{(i)} = \frac{1 + \left(\frac{\varrho_1}{\varrho^{(i)}}\right)^2}{1 - \left(\frac{\varrho_1}{\varrho^{(i)}}\right)^2}. \tag{5.16}$$

The obtained form of Eqs. (5.8)–(5.14) describing the adjoint initial problems for unknown functions $\bar{p}_0^{(i)}$ and $\bar{u}_{RC}^{(i)}$ allows — by subtracting the differential equations (5.8) and (5.12) and initial conditions (5.9), (5.13) and (5.10), (5.14) — for the formulation of an independent initial problem for the radial displacement $\bar{u}_{RC}^{(i)}$

$$\partial_\tau^2 \bar{u}_{RC}^{(i)} = \frac{1}{\bar{a}_{22}^{(i)} A^{(i)} - \frac{\bar{E}}{\varrho^{(i)}}} \left\{\partial_\tau \bar{u}_{RC}^{(i)} \left[\frac{\gamma \bar{E}}{\varrho^{(i)}} - \bar{a}_{22}^{(i)} A^{(i)} f(\tau)\right] - \bar{a}_{22}^{(i)} A^{(i)} [\partial_\tau^2 \bar{u}_R^{(i)} + \partial_\tau \bar{u}_R^{(i)} f(\tau)]\right\}, \tag{5.17}$$

$$\partial_\tau \bar{u}_{RC}^{(i)}(1) = \frac{1}{\frac{\bar{E}(1)}{\varrho^{(i)}} - \bar{a}_{22}^{(i)} A^{(i)}} \left\{ \frac{g(1)\left[\bar{a}_{21}^{(i)} + \bar{a}_{22}^{(i)} \bar{u}_R^{(i)}(1)\right] A^{(i)}}{\bar{E}(1) - \bar{a}_{22}^{(i)} A^{(i)} \varrho^{(i)}} + \right.$$

$$\left. + \bar{a}_{22}^{(i)} A^{(i)} \partial_\tau \bar{u}_R^{(i)}(1) \right\}, \tag{5.18}$$

$$\bar{u}_{RC}^{(i)}(1) = \frac{A^{(i)}}{\frac{\bar{E}(1)}{\varrho^{(i)}} - \bar{a}_{22}^{(i)} A^{(i)}} \left[\bar{a}_{21}^{(i)} + \bar{a}_{22}^{(i)} \bar{u}_R^{(i)}(1)\right], \tag{5.19}$$

where

$$A^{(i)} = D_2^{(i)} + \frac{2D_3^{(i)}}{D_1^{(i)}}. \tag{5.20}$$

In consequence of the division (Fig. 2), the particles identified with the position of prestressing cable $\varrho = \varrho^{(i)}$ belong simultaneously to the external edge of region (a) and to the hole edge of region (b) of the plate. A parallel initial problem for the function $\bar{u}_{RC}^{(i)}$ can therefore be formulated in region (b), once the stresses (4.13) are substituted into the set of Eqs. (5.4)–(5.6), at the fixed value of the radial variable $\varrho = \varrho^{(i)}$. The equations of the initial problem in the interval (b) can be found in the paper [5]. The continuity conditions for the function of radial displacement $\bar{u}_{RC}^{(i)}$ are also given in [5]. These conditions with the relations (4.7) form the set of algebraic equations wherefrom the unknown coefficients can be obtained [5].

The solution of Eqs. (5.17)–(5.19) and Eqs. (5.12)–(5.14) will be possible after determining the function $\bar{u}_R^{(i)}$ describing the action of the other prestressing cables (Fig. 3). To this end, the function $\bar{u}^{(i)}(\varrho, \tau)$ due to the action of one, arbitrarily located prestressed cable in the whole region of the plate will now be determined. As the results of substitution of the stresses (4.12) and (4.13) into Eqs. (5.4)–(5.6), the initial problems in the regions (a) and (b) will be obtained. After transformations, the problem in the region (a) ($\varrho_1 \leqslant \varrho \leqslant \varrho^{(i)}$) has the form

$$\partial^2 \bar{u}^{(i)}(\varrho, \tau) = -\gamma \partial_\tau \bar{u}^{(i)}(\varrho, \tau) + F^{(i)}(\varrho, \tau), \tag{5.21}$$

$$\partial_\tau \bar{u}^{(i)}(\varrho, 1) = \frac{\varrho}{\bar{E}(1)\left[1 - \left(\frac{\varrho_1}{\varrho^{(i)}}\right)^2\right]} \left\{ \left[\bar{r}_0^{(i)}(1) + \frac{g(1)}{\bar{E}(1)} \bar{p}_0^{(i)}(1)\right] \times \right.$$

$$\times \left[(1-\mu)\left(\frac{\varrho_1}{\varrho^{(i)}}\right)^2 + (1+\mu)\left(\frac{\varrho_1}{\varrho}\right)^2\right] - \bar{a}_{22}^{(i)}\left(\bar{v}_{RC}^{(i)}(1) + \partial_\tau \bar{u}_R^{(i)}(1)\right) +$$

$$\left. + \frac{g(1)}{\bar{E}(1)}\left[\bar{a}_{21}^{(i)} + \bar{a}_{22}^{(i)}\left(\bar{u}_{RC}^{(i)}(1) + \bar{u}_R^{(i)}(1)\right)\right]\left[(1-\mu) + (1+\mu)\left(\frac{\varrho_1}{\varrho}\right)^2\right] \right\}, \tag{5.22}$$

$$(5.23)\quad \bar{u}^{(i)}(\varrho,1)=\frac{\varrho}{\bar{E}(1)\left[1-\left(\frac{\varrho_1}{\varrho^{(i)}}\right)^2\right]}\left\{\bar{p}_0^{(i)}(1)\left[(1-\mu)\left(\frac{\varrho_1}{\varrho^{(i)}}\right)^2+\right.\right.$$

$$\left.\left.+(1+\mu)\left(\frac{\varrho_1}{\varrho}\right)^2\right]-\left[\bar{a}_{21}^{(i)}+\bar{a}_{22}^{(i)}\left(\bar{u}_{RC}^{(i)}(1)+\bar{u}_R^{(i)}(1)\right)\right]\left[1-\mu+(1+\mu)\left(\frac{\varrho_1}{\varrho}\right)^2\right]\right\},$$

where

$$(5.24)\qquad \partial_\tau \bar{p}_0^{(i)}(\varrho,\tau)=\bar{r}_0^{(i)}(\varrho,\tau),\qquad \partial_\tau \bar{u}_{RC}^{(i)}(\varrho,\tau)=\bar{v}_{RC}^{(i)}(\varrho,\tau).$$

To simplify the differential Eqs. (5.21)–(5.23), the following notation has been introduced:

$$(5.25)\quad F^{(i)}(\varrho,\tau)=\frac{2\varrho}{\bar{E}}f(\tau)\,\bar{r}_0^{(i)}\left[(1-\mu)\left(\frac{\varrho_1}{\varrho^{(i)}}\right)^2+(1+\mu)\left(\frac{\varrho_1}{\varrho}\right)^2\right]-$$

$$-\frac{\bar{a}_{22}^{(i)}\varrho}{\bar{a}_{22}^{(i)}A^{(i)}\varrho^{(i)}-\bar{E}}\left[\bar{v}_{RC}^{(i)}(\gamma-f(\tau))-\partial_\tau^2\,\bar{u}_R^{(i)}-f(\tau)\,\partial_\tau\,\bar{u}_R^{(i)}\right]\times$$

$$\times\left\{\frac{2}{D_1^{(i)}}\left[(1-\mu)\left(\frac{\varrho_1}{\varrho^{(i)}}\right)^2+(1+\mu)\left(\frac{\varrho_1}{\varrho}\right)^2\right]-(1-\mu)-(1+\mu)\left(\frac{\varrho_1}{\varrho}\right)^2\right\}.$$

The above set of equations describing the disc state of the plate subject to the action of an arbitrarily chosen i-th cable contains the unknown function $\bar{u}_R^{(i)}(\tau)$. To calculate the function $\bar{u}_R^{(i)}$, the iterative procedure discussed in the paper [5] should be applied.

The analytical solution for the displacement function can be obtained by neglecting the phenomenon of ageing in the description of material properties. The kernel form (5.1) of the physical equation in that case may be obtained by substituting into the formulae (5.2) the boundary magnitudes of the ageing function $\bar{\varphi}(\tau)$ and Young's modulus $\bar{E}(\tau)$ at $\tau\to\infty$. According to the algorithm given earlier, the displacement $\bar{u}_{RC}^{(i)}$ and reaction pressure $\bar{p}_0^{(i)}$ should be determined first. In this manner, the initial problems formulated at points $\varrho=\varrho_1$ and $\varrho=\varrho^{(i)}$ (by analogy with Eqs. (5.8)–(5.10) and (5.12)–(5.14)) enable us to obtain the analytical solutions for the functions $\bar{u}_{RC}^{(i)}$ and $\bar{p}_0^{(i)}$. In particular, the radial displacement $\bar{u}_{RC}^{(i)}$ has the form given in paper [5], whereas the function of reaction pressure can be written as

$$(5.26)\quad p_0^{(i)}(\tau)=p_0^{(i)}(1)\,e^{-\delta(\tau-1)}+\frac{2}{D_1^{(i)}}\left\{\frac{B_1^{(i)}}{\delta-L^{(i)}}\left[e^{-L^{(i)}(\tau-1)}+e^{-\delta(\tau-1)}\right]+\right.$$

$$+\frac{B_5^{(i)}}{\delta}\left[1-e^{-\delta(\tau-1)}\right]+B_3^{(i)}\left[\bar{u}_R^{(i)}(\tau)-\bar{u}_R^{(i)}(1)\,e^{-\delta(\tau-1)}\right]+$$

$$\left.+(B_2^{(i)}-\delta B_3^{(i)})\,e^{-\delta\tau}\int_1^\tau \bar{u}_R^{(i)}(\tau)e^{\delta\tau}+B_4^{(i)}e^{-\delta\tau}\int_1^\tau e^{(\delta-L^{(i)})\tau}\left[\int_1^\tau \bar{u}_R^{(i)}(\tau)\,e^{-L^{(i)}\tau}\,d\tau\right]d\tau\right\},$$

where

$$\delta = \gamma\,(1 - C_0\,E\,(1)). \tag{5.27}$$

The instantaneous reaction pressure $\bar{p}_0^{(i)}(1)$ is determined by the relation (5.10); however, the coefficients $L^{(i)}$, $M^{(i)}$ and $B_j^{(i)}$ for $j = 1, 2, \ldots, 5$ are given in [5].

The solution of the initial problem with respect to the displacement $\bar{u}^{(i)}(\varrho, \tau)$ is shown in paper [5]. Nevertheless, in the present paper the functions $K_j^{(i)}$ for the region (a) should be taken as follows:

$$K_j^{(i)}(\varrho) = \frac{\varrho}{\bar{E}\,(1)\,D_1^{(i)}}\,(1-\mu^2)\left[1-\left(\frac{\varrho_1}{\varrho}\right)^2\right] B_j^{(i)}. \tag{5.28}$$

The calculated components of the radial displacement vector $\bar{u}_{RC}^{(i)}(\tau)$, $\bar{u}_R^{(i)}(\tau)$ and the reaction pressure $\bar{p}_0^{(i)}(\tau)$ allow to determine the radial and circumferential stresses according to the relations (4.12) and (4.13). The function of the disc stresses of the plate prestressed n-times will be calculated by means of the principle of superposition

$$s_\varrho^T = \sum_{i=1}^{n} s_\varrho^{(i)}, \qquad s_\theta^T = \sum_{i=1}^{n} s_\theta^{(i)}. \tag{5.29}$$

6. Iterative solution of the plate equation

As we know, there exists no general method of solving the differential-functional Eq. (3.8). In order to present the iterative method proposed, Eq. (3.8) will be written in the form

$$\nabla^2\,\nabla^2\,\bar{w} = \frac{3}{4}\,(1-\mu)\,L_c\left[\bar{q} + \frac{2}{\varrho}\,s_\theta^T\,\langle \bar{w}_{,\varrho}\rangle + 2 s_\varrho^T\,\langle \bar{w}_{,\varrho\varrho}\rangle\right]. \tag{6.1}$$

Triangular brackets contain the expressions which appear in the plate equation in consequence of rejection of the stiffness principle. These expressions take into account the influence of eccentricity of the disc stress on the plate deflection $\bar{w}(\varrho, \tau)$.

As far as the kinematic boundary conditions are concerned, one should not expect large changes in deflections caused by the disc stresses. However, the changes of deflection lead to considerable redistribution of the plate stresses. Let us now take into account the stiffness principle and calculate the deflection $\bar{w}(\varrho, \tau)$ of the plate. Initially the disc stresses will be disregarded ($s_\varrho^T = s_\theta^T = 0$), and the first approximation of $\bar{w}(\varrho, \tau)$ will be the solution of the equation

$$\nabla^2\,\nabla^2\,\bar{w}(\varrho, \tau) = \frac{3}{4}\,(1-\mu)\,L_c(\bar{q}), \tag{6.2}$$

with the boundary conditions (Fig. 1):

for the fixed age ($\varrho = \varrho_1$)

$$\bar{w}_{,\varrho}(\varrho_1, \tau) = 0, \tag{6.3}$$

$$\bar{w}(\varrho_1, \tau) = 0; \tag{6.4}$$

and for the free edge ($\varrho = \varrho_2$)

$$m_\varrho(\varrho_2, \tau) = 0 \underset{(3.3)}{\Longrightarrow} \left(\bar{w}_{,\varrho\varrho} + \frac{\mu}{\varrho}\bar{w}_{,\varrho}\right)\Big|_{(\varrho=\varrho_2,\,\tau)} = 0, \tag{6.5}$$

$$q_\varrho(\varrho_2, \tau) = 0 \underset{(3.6)}{\Longrightarrow} \left[\frac{2}{3(1-\mu)}(\nabla^2 \bar{w})_{,\varrho} + L_c(s_\varrho^T \bar{w}_{,\varrho})\right]\Big|_{(\varrho=\varrho_2,\,\tau)} = 0. \tag{6.6}$$

The function $\bar{w}(\varrho, \tau)$ calculated in the first approximation is introduced to the expressions in triangular brackets of Eq. (6.1). The second approximation ($j = 2$) follows from the solution of the equation

$$\nabla^2 \nabla^2 \bar{w}(\varrho, \tau) = \frac{3}{4}(1-\mu) L_c(\bar{q}^{(j)}) \tag{6.7}$$

with the known nonhomogeneity

$$\bar{q}^{(j)} = \bar{q} + \frac{2}{\varrho} s_\theta^T \langle \bar{w}_{,\varrho} \rangle + 2 s_\varrho^T \langle \bar{w}_{,\varrho\varrho} \rangle. \tag{6.8}$$

The third and further approximations ($j = 3, 4, \ldots$) result from the solution of Eq. (6.7) with the boundary conditions (6.3)–(6.6), while in the expression (6.8) the magnitude $\bar{w}(\varrho, \tau)$ calculated in the previous iteration is used. This procedure is repeated until the differences between the succesive approximations become comparable with the error of numerical integration.

According to the criterion of restricted prestressing, tensile stresses in the material should not be greater than the admissible values Δs. This condition for cantilever plate can be written in the form of inequalities:

$$s_\varrho^T(\varrho_1, \tau) + s_\varrho(\varrho_1, \xi = -1, \tau) \leqslant \Delta s, \tag{6.9}$$

$$s_\theta^T(\varrho_x, \tau) + s_\theta(\varrho_x, \xi = -1, \tau) \leqslant \Delta s, \tag{6.10}$$

where s_ϱ and s_θ are the plate stresses, the magnitudes of which are expressed by the function of deflection in view of Eqs. (3.3), (3.4) and (3.5). The radial coordinate ϱ_x is connected with the maximum of circumferential moments (3.4).

The finite differences method has been applied in numerical solution of the iterative problem (6.7), (6.3)–(6.6). Convergence of the iterative algorithm is found to be good. The differences between the second and third approximations are smaller than 1%.

In the numerical analysis of creep process of the plate shown below, the material constants will be taken as follows:

$$C_0 = 3.6\cdot 10^{-3}, \quad E_0 = 6.25\cdot 10^2, \quad A = 6.85\cdot 10^{-4}, \tag{6.11}$$
$$\alpha = 1.4, \quad \beta = 0.6, \quad \gamma = 0.728,$$

These data correspond to the creep behaviour typical for concretes made from Portland cement.

As an example, consider the prestressed plate (Fig. 1) with six cables and $\varrho_1 = 2.5$ and $\varrho_2 = 17.5$. The cable routes coincide with circles of radii: $\varrho^{(1)} = 5$, $\varrho^{(2)} = 7.5$, $\varrho^{(3)} = 10$, $\varrho^{(4)} = 12.5$, $\varrho^{(5)} = 15$, $\varrho^{(6)} = 17.5$. The prestressing is characterized by the magnitudes

$$\bar{a}_1^{(1)} = \bar{a}_1^{(2)} = \bar{a}_1^{(3)} = \bar{a}_1^{(4)} = \bar{a}_1^{(5)} = \bar{a}_1^{(6)} = 0.05,$$
$$\bar{a}_2^{(1)} = 6, \quad \bar{a}_2^{(2)} = 4, \quad \bar{a}_2^{(3)} = 3, \quad \bar{a}_2^{(4)} = 2.4, \quad \bar{a}_2^{(5)} = 2, \quad \bar{a}_2^{(6)} = 1.72. \tag{6.12}$$

The radial s_ϱ and circumferential stresses s_θ at the upper surface ($\xi = -1$) of the uniformly loaded plate ($\bar{q} = 1.25\cdot 10^{-4}$), for the material function (5.1), are presented in Figs. 4 and 5. Solid lines illustrate the solution in which the stiffness principle is disregarded (6.1), contrary to the centre lines

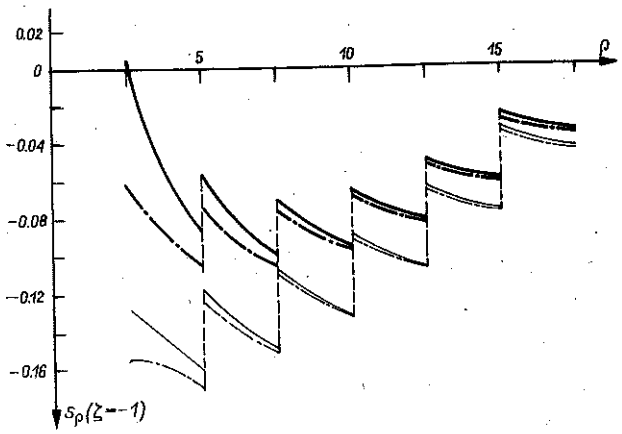

FIG. 4.

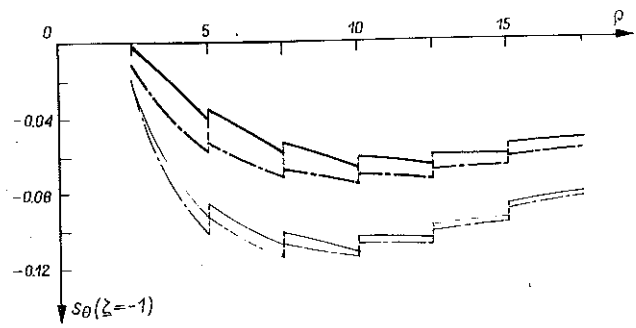

FIG. 5.

where this principle is included (6.2); the influence of the disc stresses on the plate deflection is disregarded. At the same time, light lines concern the functions at the instant ($\tau = 1$), while heavy lines show their shape at the instant $\tau = 6$, when the creep process is finished. The stress discontinuities appearing at the points of location of the cables are marked by dashed lines.

The stress redistribution caused by the loss of prestressing during creep may lead to tensile stresses in some regions of the plate. In the case of the considered cantilever plate, such a possibility takes place for both the radial and circumferential stresses. In particular, for the assumed method of prestressing (6.12), the radial stresses change their sign and do not exceed the admissible magnitude Δs at time $\tau = 6$ (heavy solid line for $\varrho = 2.5$), Fig. 4. The figure shows that the effect of disadvantageous stress redistribution may be neglected in calculation provided the stiffness principle is assumed (heavy centre line for $\varrho = 2.5$).

The changes of radial and circumferential stresses plotted against time τ of creep at the upper surface of the plate $\zeta = -1$ and $\varrho = 2.5$ are shown in Figs. 6 and 7. From the asymptotic behaviour of these functions it follows that, after time $\tau = 6$, no further changes in the stress distribution appear. Solid lines illustrate the functions corresponding to three different values of the uniform load $\bar{q}$. The other curves show the shape of the function for $\bar{q} = 1.25 \cdot 10^{-4}$ under the simplifying assumptions: the stiffness principle (centre lines) no cable interactions $\bar{u}_R^{(i)}(\tau) = 0$ (dashed lines) and nonageing model of the material (doted lines). The analogous graphical convention is applied in Fig. 8 where the relative deflection as a function of time τ for the load $\bar{q} = 1.25 \cdot 10^{-4}$ is presented.

The relative deflection at the midspan referred to the instantaneous deflection of the edge $\varrho = \varrho_2$ (for $\bar{q} = 1.25 \cdot 10^{-4}$) is shown in Fig. 9. Solid lines, light and heavy, are connected with the respective deflections for $\tau = 1$ and $\tau = 6$. Disregarding of the cable interaction in the disc state $\bar{u}_R^{(i)}(\tau) = 0$ leads to an additional loading caused by change of prestressing, and thus to a greater deflection (dashed line for $\tau = 6$). If the influence of the disc state on the state of bending of the plate (6.2) is disregarded, the deflections are smaller (centre line for $\tau = 6$).

From the comparison of the formulae (6.1) and (6.2), it follows that the omission of the stiffness principle is formally equivalent to the additional load $\bar{q}^T$ in the plate equation

$$\bar{q}^T = \frac{2}{\varrho} s_\vartheta^T \bar{w}_{,\varrho} + 2 s_\varrho^T \bar{w}_{,\varrho\varrho}. \tag{6.13}$$

This function (for the useful load $\bar{q} = 1.25 \cdot 10^{-4}$) is presented in Fig. 10. Solid lines, light and heavy, correspond to instants $\tau = 1$ and $\tau = 6$. The

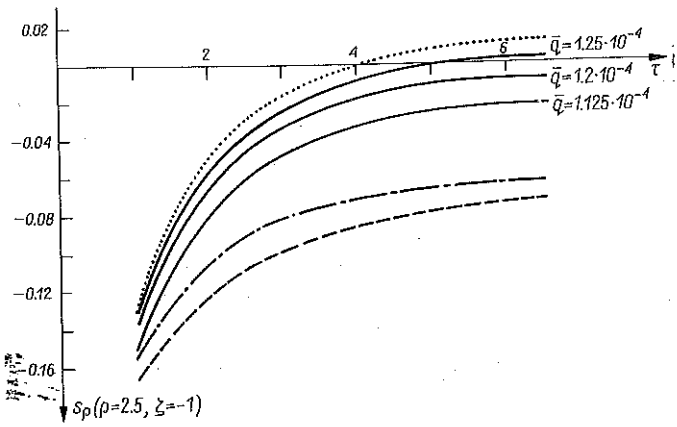

FIG. 6.

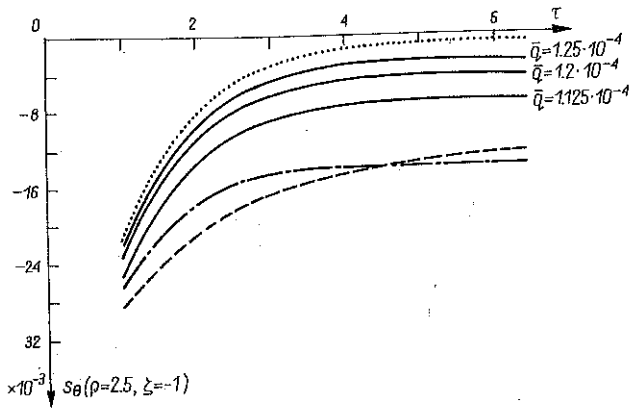

FIG. 7.

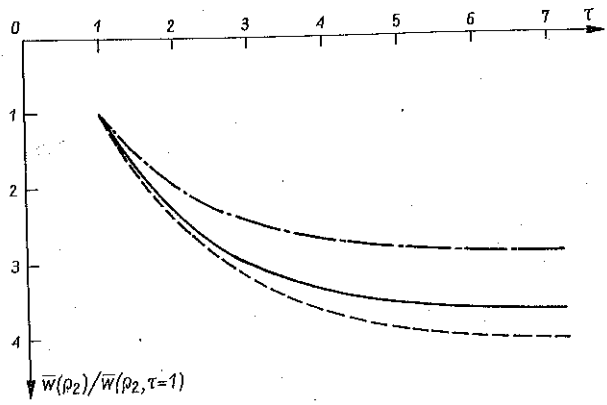

FIG. 8.

increase of the additional load $\bar{q}^T$ will take place if, in the solution of the disc state, the interaction of cables is neglected, $\bar{u}_R^{(i)} = 0$ (dashed lines).

The applied constitutive relation of linear visco-elasticity is valid for stresses smaller than 50 per cent of the ultimate strength of the concrete.

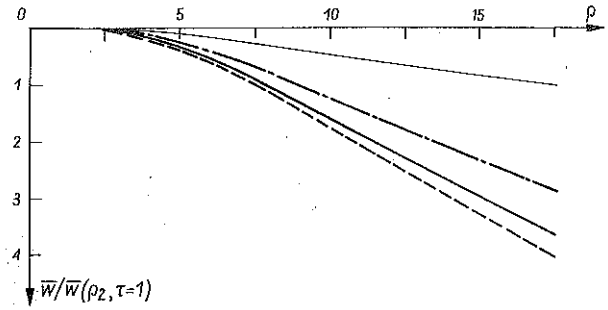

FIG. 9.

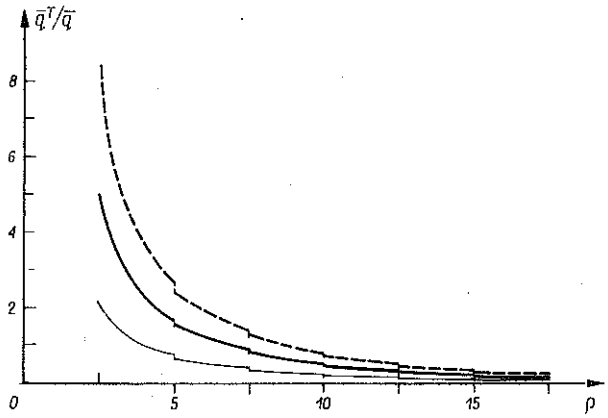

FIG. 10.

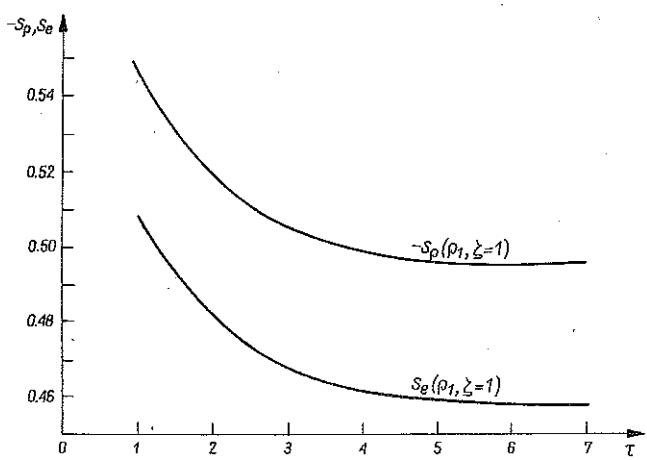

FIG. 11.

In the case of plates, this condition is related to the reduced stress, calculated according to the von Mises hypothesis:

$$s_e = (s_\varrho^2 - s_\varrho\, s_\theta + s_\theta^2)^{1/2} \leqslant 0.5. \tag{6.14}$$

The reduced stress function (at the lower surface of the plate $\zeta = 1$ and at a fixed point $\varrho = \varrho_1$), and radial stresses plotted against time τ, are presented in Fig. 11.

7. Final remarks

The method of the solution presented in this paper makes it possible to carry out the creep analysis for any prestressing program determined by technological conditions. In programming the digital computer, one should take into account the properties of the material of the plate, the operation of prestressing and the sequence of stretching of the prestressing cables. These data connected with the time scale are the steering magnitudes for the calculation programme. The numerical example solved in the preceding chapter shows the creep process of the plate, under the initial conditions formulated for simultaneous application of both the load and prestressing.

Similarly as in the case of prestressed discs [5], disregarding of the ageing effect in the description of the material properties increases the loss of prestressing (doted lines, Figs. 6 and 7). This indicates that the nonageing model leads to a safer design.

The mechanical properties are represented by the nonlinear degenerated function (5.1). This assumption does not limit the practical possibilities of applying the method of solution shown above. According to the Mercer theorem [17], all kernels having a norm can be written as

$$K(\tau, \tau') = \sum_{i=1}^{\infty} f_i(\tau)\, g_i(\tau'). \tag{7.1}$$

In practical calculations, the sum of a finite number of products (7.1) is taken [18], what enables to replace the given kernel approximately by a degenerate function.

References

1. A. Ajdukiewicz, J. Mames, *Prestressed constructions*, PWN, Warszawa 1976 [in Polish].
2. K. Grabiec, J. Kampioni, *Concrete prestressed constructions*, PWN, Warszawa 1982 [in Polish].
3. J. Biliszczuk, *Rheological redistribution of the state of stresses in heterogeneous isostatical concrete structures*, PWN, Warszawa 1982 [in Polish].
4. R. Atallah, M. Brachet, G. Darpas, *Contribution a l'estimation des pertes precontrainte et des deformations differees des structures en beton precontraint*, VII Congres de la FIP, New York 1974.
5. J. Białkiewicz, *Rheology of prestressed circularly symmetric discs*, Eng. Trans., **32**, 4, 1983.
6. W. Marks, *Optimization of stretched bending elements*, IFTR Reports, Warszawa 1978 [in Polish].

7. P. PERZYNA, *Thermodynamics of non-elastic materials*, PWN, Warszawa 1978 [in Polish].
8. R. M. CHRISTENSEN, *Theory of viscoelasticity*, Ac. Press, New York, London 1974.
9. S. TIMOSHENKO, S. WOJNOWSKY-KRIEGER, *Theory of plates and shells*, Mc Graw-Hill Book Comp., New York 1959.
10. Z. KĄCZKOWSKI, *Plates-statical calculations*, Arkady, Warszawa 1980 [in Polish].
11. J. BIAŁKIEWICZ, S. PIECHNIK, *Creep of concrete ring disc*, Czasop. Techn., Pol. Krak., 7-B, (214), 1978 [in Polish].
12. D. E. BRANSON, M. L. CHRISTIASON, *Time dependent concrete properties related to design*, ACI, 27, Detroit 1971.
13. N. ARUTYNYAN, *Some problems in the theory of creep*, [trans. by H. E. Nowottny], Pergamon Press, 1966.
14. J. N. MADSEN, *Practical calculation of creep and shrinkage of concrete in terms of a matrix formulation*, Nordisk Betong, 1, 1979.
15. B. CIVIDINI, *Long-term deflection of aerated reinforced concrete slabs*, Int. J. Cem. Comp., 3, 3, 1981.
16. M. KAWASUMI, S. SEKI, K. KASAHARA, T. KURIYAMA, *A constitutive creep law of concrete with particular reference to its internal structure and hydration of cement*, IUTAM Symp., Leicester 1980.
17. G. A. KORN, T. M. KORN, *Mathematical handbook*, McGraw-Hill, 1968.
18. M. KRASNOV, A. KISELEV, G. MAKARENKO, *Problems and exercises in integral equations*, MIR, Moscow 1971.

STRESZCZENIE

STAN NAPRĘŻENIA WE WSTĘPNIE SPRĘŻONEJ PŁYCIE PIERŚCIENIOWEJ W WARUNKACH PEŁZANIA

Przedstawiono rozwiązanie zagadnienia pełzania płyty pierścieniowej sprężonej wstępnie układem kabli koncentrycznych. Metoda rozwiązania oparta jest na podwójnym algorytmie iteracyjnym. W sposób iteracyjny rozwiązano zagadnienie współdziałania cięgien sprężających, jak również problem wpływu tarczowego stanu naprężenia w płycie na stan naprężenia przy zginaniu.

РЕЗЮМЕ

НАПРЯЖЕННОЕ СОСТОЯНИЕ В ПРЕДВАРИТЕЛЬНО НАПРЯЖЕННОЙ КОЛЬЦЕВОЙ ПЛИТЕ В УСЛОВИЯХ ПОЛЗУЧЕСТИ

Представлено решение задачи ползучести кольцевой плиты, предварительно напряженной системой концентрических кабелей. Метод решения опирается на двойном итерационном алгоритме. Итерационным способом решена задача взаимодействия напряжающих связей, как тоже задача влияния дискового напряженного состояния в плите на напряженное состояние при изгибе.

DEPARTMENT OF CIVIL ENGINEERING
TECHNICAL UNIVERSITY OF CRACOW.

Received November 11, 1984.